Stationary distributions of propelled particles as a system with quenched disorder

Derek Frydel
Department of Chemistry, Universidad Técnica Federico Santa María, Campus San Joaquin, Santiago 8940572, Chile

(Received 25 January 2021; accepted 20 April 2021; published 5 May 2021)

This article is the exploration of the viewpoint within which propelled particles in a steady state are regarded as a system with quenched disorder. The analogy is exact when the rate of the drift orientation vanishes and the linear potential, representing the drift, becomes part of an external potential, resulting in the effective potential $u_{\rm eff}$. The stationary distribution is then calculated as a disorder-averaged quantity by considering all contributing drift orientations. To extend this viewpoint to the case when a drift orientation evolves in time, we reformulate the relevant Fokker-Planck equation as a self-consistent relation. One interesting aspect of this formulation is that it is represented in terms of the Boltzmann factor $e^{-\beta u_{\rm eff}}$. In the case of a run-and-tumble model, the formulation reveals an effective interaction between particles.

DOI: 10.1103/PhysRevE.103.052603

I. INTRODUCTION

Within the two standard models of propelled motion, the run-and-tumble (RTP) and active Brownian particle (ABP) model, particles are subject to a drift of constant magnitude v_0 but randomized orientation. The time evolution of the drift is what prevents a system from attaining an equilibrium. The evolution of the orientation in each model is governed by a different stochastic process. In the RTP model, the new direction is assigned sporadically at intervals drawn from Poisson distribution. A new orientation can take on any value with equal probability. In the ABP model, the orientation undergoes diffusion. The rate of orientation change in the RTP model is α, and the angular diffusion in the ABP model is D_r.

Despite the apparent simplicity of an ideal-gas model of propelled particles, there is no available analytical solution for stationary distributions. One noted exception is the RTP model in one dimension with drift limited to two values, $v = \pm v_0$ [1–7]. Yet even a simple extension to three drifts $v = 0, \pm v_0$ leads to considerable increase in complexity [8]. (The third model of propelled motion is the active Ornstein Uhlenbeck particles, AOUP [9,10]; however, in this work we exclusively focus on the RTP and ABP models.)

In this work, we take a different point of view to characterize stationary distributions of propelled particles. We start by considering a stationary state of propelled particles at exactly $\alpha = D_r = 0$. Under these conditions, the unit vector $\mathbf{u}_v$, representing orientation of a drift, stops evolving in time and as a consequence the system attains equilibrium. The result is a mixture of particles with different drift orientations. And because the drift orientations are randomly distributed, the situation corresponds to a system with quenched disorder. The stationary distribution is a disorder-averaged distribution that takes into account all drift orientations.

The resulting distribution for the condition $\alpha = D_r = 0$ represents the largest deviation from the distribution for the same system but for passive Brownian particles. Since in the limit $\alpha \to \infty$ and/or $D_r \to \infty$ the distribution converges to that of passive particles, this limit is generally regarded as representing an equilibrium. The suggestion, therefore, that the opposite limit $\alpha, D_r \to 0$ corresponds to an equilibrium appears to contradict this view. If we look into the entropy production Π that is used as a quantification of distance from the equilibrium, we find that Π vanishes as $\alpha, D_r \to 0$, supporting the claim that this limit represents an equilibrium. The opposite limit $\alpha \to \infty$ is found to yield the largest possible value of Π, indicating the largest deviations from equilibrium—a surprising result given that the distribution in that limit is the same as that for passive Brownian particles.

The central quantity that emerges in analyzing the limit $\alpha, D_r \to 0$ is the effective external potential, which is the original external potential $u_{\rm ext}$ plus the linear potential representing a drift, $u_{\rm eff} = u_{\rm ext} + [\mathbf{u}_v \cdot \mathbf{r}]v_0/D$. One way to go beyond the decoupled limit is to expand the stationary distribution perturbatively as $n \approx n_0 + \alpha n_1$. This approach, however, leads to a rather complex expression for n_1 without offering valuable insights. Instead, we reformulate the stationary Fokker-Planck equation (FP) as a self-consistent relation (SC). The central quantity of the SC formulation is the Boltzmann factor $e^{-\beta u_{\rm eff}}$. Within the SC formulation, propelled particles appear as if they were coupled, but the effective attraction has the "chemical" origin and arises when particles of different drift orientations are regarded as different species that undergo a continuous conversion. The SC formulation is used as a basis for numerical computation of stationary distributions, an alternative procedure to dynamic simulations.

This work is organized as follows. In Sec. II we introduce a general FP equation of propelled particles for an arbitrary dimension d. In Sec. III we consider exact distributions for a decoupled condition $\alpha = D_r = 0$, which represents the system with quenched disorder. In Sec. IV we develop the self-consistent framework for solving the stationary FP equation. The goal of such a framework is to gain insights as well as to look for alternative numerical schemes other than dynamic simulations. In Sec. V we analyze the entropy production of a two-state RTP model.

II. THEORETICAL FRAMEWORK

The motion of an ideal gas of propelled particles in a general d-dimensional space, with both RTP and ABP type of motion, is governed by the following Fokker-Planck equation (FP):

$$\frac{\partial n}{\partial t} = D\nabla^2 n - v_0 \mathbf{u}_v \cdot \nabla n + \beta D \nabla \cdot [n \nabla u_{\rm ext}] - \alpha\left[n - \frac{1}{\Omega_v}\int d\Omega_v\, n\right] + D_r \hat{L}_S n, \tag{1}$$

where the distribution $n \equiv n(\mathbf{r}, \mathbf{u}_v, t)$ is the function of the position $\mathbf{r}$, drift orientation $\mathbf{u}_v$ ($\mathbf{u}_v$ is a unit vector), and time t, and is normalized to unity as $\int d\mathbf{r}\, n(\mathbf{r}, \mathbf{u}_v, t) = 1$. The first line in Eq. (1) governs the evolution of particle positions and involves standard diffusion, drift of constant magnitude v_0, and the interaction with external forces due to a conservative potential $u_{\rm ext}(\mathbf{r})$.

The second line in Eq. (1) governs the evolution of the unit vector $\mathbf{u}_v$, which determines the orientation of a drift. The time evolution of $\mathbf{u}_v$ is what prevents the system from attaining equilibrium. The first term gives rise to the RTP type of motion, where $\Omega_v = \int d\Omega_v$ is the area of a unit sphere in a given dimension. The RTP motion is represented as a "reaction" process where particles of different orientations are continuously created and destroyed yet their total number is conserved. The ABP motion is represented as a diffusion of a unit vector $\mathbf{u}_v$ on a surface of a sphere, and the operator $\hat{L}_S$ is a spherical Laplacian operator on the $(d-1)$ sphere.

For the explicit dimension $d = 2$ the second line in Eq. (1) becomes

$$\frac{\partial n}{\partial t} = -\nabla \cdot \mathbf{j} - \alpha\left[n - \frac{1}{2\pi}\int_0^{2\pi} d\theta_v\, n\right] + D_r \frac{\partial^2 n}{\partial \theta_v^2}, \tag{2}$$

where we introduce the flux

$$\mathbf{j}(\mathbf{r}, \mathbf{u}_v) = -D\nabla n + v_0 \mathbf{u}_v n - \beta D \nabla \cdot [n \nabla u_{\rm ext}].$$

Because Eqs. (1) and (2) involve creation-destruction of particles with different orientations, it is not immediately clear if the total number of particles is conserved. To demonstrate that this is the case, we integrate Eq. (2) over the space domain within which the system is confined,

$$\frac{\partial N}{\partial t} = -\alpha\left[N - \frac{1}{\Omega_v}\int d\Omega_v\, N\right] + D_r \frac{\partial^2 N}{\partial \theta_v^2}, \tag{3}$$

where we define the number of particles with particular orientation as $N(\mathbf{u}_v) = \int d\mathbf{r}\, n(\mathbf{r}, \mathbf{u}_v)$. Note that $\int d\mathbf{r}\, \nabla \cdot \mathbf{j} = 0$, since particles do not enter or leave the prescribed domain. Finally, if we integrate Eq. (3) over all orientations and define $\bar{N} = \frac{1}{\Omega_v}\int d\Omega_v\, N(\mathbf{u}_v)$, we have

$$\frac{\partial \bar{N}}{\partial t} = -\alpha[\bar{N} - \bar{N}] + D_r\left[\frac{\partial N}{\partial \theta_v}\right]_0^{2\pi} = 0, \tag{4}$$

where the second term cancels out as a result of periodic boundary conditions. The total number of particles, therefore, is conserved.

At this point we introduce the "effective" external potential, defined as

$$\beta u_{\rm eff} = \beta u_{\rm ext} - \frac{v_0}{D}[\mathbf{u}_v \cdot \mathbf{r}], \tag{5}$$

which is the external potential plus the linear potential for representing a drift. As we limit our analysis to stationary distributions, the time-independent FP equation of interest is

$$0 = D\nabla^2 n + \beta D \nabla \cdot [n \nabla u_{\rm eff}] - \alpha\left[n - \frac{1}{\Omega_v}\int d\Omega_v\, n\right] + D_r \hat{L}_S n. \tag{6}$$

The stationary distribution that accounts for all orientations is defined as

$$\bar{n}(\mathbf{r}) = \frac{1}{\Omega_v}\int d\Omega_v\, n(\mathbf{r}, \mathbf{u}_v),$$

where the bar indicates the averaging procedure.

III. EXACT TREATMENT IN A DECOUPLED LIMIT, $\alpha = 0$ AND $D_r = 0$

In this section we obtain distributions n for a decoupled condition given by $\alpha = D_r = 0$. Because under such circumstances $\mathbf{u}_v$ stops to evolve in time, the system is in equilibrium, but the distribution of drift orientations introduces quenched disorder.

By setting both α and D_r to zero, Eq. (6) reduces to

$$0 = D\nabla^2 n_0 + \beta D \nabla \cdot [n_0 \nabla u_{\rm eff}]. \tag{7}$$

The result is the standard diffusion equation for a particle in the external potential $u_{\rm eff}$. The solution is proportional to the Boltzmann weight,

$$n_0(\mathbf{r}, \mathbf{u}_v) \propto e^{-\beta u_{\rm ext}} e^{[\mathbf{u}_v \cdot \mathbf{r}] v_0 / D}.$$

The subscript "0" is used to indicate that the solution is true only for the case $\alpha = D_r = 0$. The actual stationary distribution is obtained by averaging over all possible drifts $\mathbf{u}_v$ uniformly distributed over all orientations and given by

$$\bar{n}_0(\mathbf{r}) \propto \int d\Omega_v\, e^{-\beta u_{\rm ext} + [\mathbf{r} \cdot \mathbf{u}_v] v_0 / D}. \tag{8}$$

Quenched disorder is the inherent feature of the system in the decoupled limit.

If $u_{\rm ext}$ depends on particle positions only, then the Boltzmann factor can be separated and the above equation can be written as

$$\bar{n}_0(\mathbf{r}) \propto e^{-\beta u_{\rm ext}(\mathbf{r})} \int d\Omega_v\, e^{[\mathbf{r} \cdot \mathbf{u}_v] v_0 / D}.$$

All orientations in the above formulation are equally likely, and there is no bias for any particular direction. But if the external potential contributes to particle orientations, $u_{\rm ext} \equiv u_{\rm ext}(\mathbf{r}, \mathbf{u}_v)$, a case that might arise for particles with dipole moment, the orientation would no longer be distributed uniformly and we would have

$$\bar{n}_0(\mathbf{r}) \propto \int d\Omega_v\, e^{-\beta u_{\rm ext}(\mathbf{r}, \mathbf{u}_v)} e^{[\mathbf{r} \cdot \mathbf{u}_v] v_0 / D}.$$

Such orientation bias would reduce quenched disorder. In this work, however, we limit our interest to the position-dependent potentials.

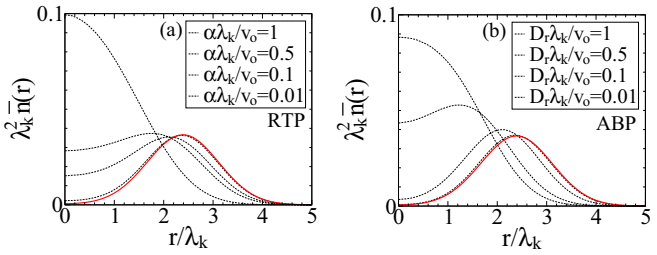

FIG. 1. Distributions of propelled particles in the potential $u_{\rm ext} = Kr^2/2$ obtained from dynamic simulations for $d = 2$ (dashed black lines). $\lambda_k = \sqrt{2/\beta K}$ is the trap size, and the results are for $v_0\lambda_k/D = 5$. The solid red line corresponds to the expression in (10). The results in (a) are for RTP and those in (b) for ABP type of motion.

A. Harmonic trap

We next consider a number of specific potentials. For a harmonic potential $\beta u_{\rm ext} = \frac{1}{2}Kr^2$, $u_{\rm eff} = \frac{1}{2}Kr^2 - [\mathbf{u}_v \cdot \mathbf{r}]v_0/D$ and the Boltzmann distribution representing the decoupled limit is

$$n_0(\mathbf{r}, \mathbf{u}_v) \propto e^{-\frac{1}{2}\beta K r^2} e^{[\mathbf{u}_v \cdot \mathbf{r}]v_0/D}. \tag{9}$$

The disorder-averaged distribution is obtained using Eq. (8). For dimension $d = 2$ we have $d\Omega_v = d\theta_v$, leading to

$$\bar{n}_0(r) \propto e^{-\frac{1}{2}\beta K r^2} \int_0^{2\pi} d\theta_v \, e^{r\cos\theta_v v_0/D}.$$

After evaluating the integral we find

$$\bar{n}_0(r) = \left[\left(\frac{\beta K}{2\pi}\right) e^{-\frac{1}{2}\beta K r^2}\right]\left[e^{-\frac{v_0^2}{2D^2\beta K}} I_0\left(\frac{v_0 r}{D}\right)\right]. \tag{10}$$

The two terms in square brackets indicate different contributions. The first is the usual Gaussian distribution for passive particles in a harmonic potential. The second term, represented by the modified Bessel function $I_0(x)$, is the contribution due to propelled motion. This term diverges far away from the center of the trap as $I_0(x) \approx e^x/\sqrt{2\pi x}$ and gives rise to particle deposition at the border of a trap [11].

For dimension $d = 3$, the drift orientation is uniformly distributed on a unit sphere with $d\Omega_v = \sin\theta_v d\theta_v d\phi_v$. The disorder-averaged distribution obtained using Eq. (8) is

$$\bar{n}_0(r) \propto e^{-\frac{1}{2}\beta K r^2} \int_0^{2\pi} d\phi_v \int_0^{\pi} d\theta_v \, \sin\theta_v \, e^{r\cos\theta_v v_0/D}$$

and evaluates to

$$\bar{n}_0(r) = \left[\left(\frac{\beta K}{2\pi}\right)^{3/2} e^{-\frac{1}{2}\beta K r^2}\right]\left[e^{-\frac{v_0^2}{2D^2\beta K}} \frac{D}{v_0 r} \sinh\left(\frac{v_0 r}{D}\right)\right]. \tag{11}$$

The result is similar to that in Eq. (10). The deposition of particles predicted by (10) and (11) correspond to the optimal deposition. Any finite value of $\alpha > 0$ or $D_r > 0$ would make this deposition less extreme. To see how the true stationary distributions $\bar{n}(r)$ evolve toward $\bar{n}_0(r)$ as α or D_r tend to zero, in Fig. 1 we plot the distributions obtained from dynamic simulations for both the RTP and ABP type of motion for particles trapped in the harmonic potential and for the dimension $d = 2$. The results are compared to the limiting functional form in Eq. (10).

B. Particles in a confinement with 1D geometry

If a confining potential has one-dimensional (1D) geometry, the system is effectively 1D. The simplest example is for particles trapped between two parallel walls. Since $u_{\rm ext} = 0$, the effective potential is

$$\beta u_{\rm eff}(x) = -\frac{v_x x}{D},$$

where x axis is perpendicular to the walls.

The normalized Boltzmann distribution for this effective potential, representing the decoupled limit, is

$$n_0(x, v_x) = \frac{1}{2h}\frac{v_x h}{D}\frac{e^{\frac{v_x x}{D}}}{\sinh\left(\frac{v_x h}{D}\right)}. \tag{12}$$

For the dimension $d = 2$ the disorder-averaged distribution is given by

$$\bar{n}_0(x) = \frac{1}{2\pi}\int_0^{2\pi} d\theta_v \, n_0(x, v_0\cos\theta_v). \tag{13}$$

Using $\frac{d\cos\theta_v}{d\theta_v} = -\sin\theta_v$ and $v_x = v_0\cos\theta_v$, we obtain

$$d\theta_v = -\frac{dv_x}{\sqrt{v_0^2 - v_x^2}},$$

and the integral in Eq. (12) can be rewritten as

$$\bar{n}_0(x) = \frac{1}{\pi}\int_{-v_0}^{v_0} dv_x \frac{n_0(x, v_x)}{\sqrt{v_0^2 - v_x^2}}. \tag{14}$$

Or more generally, we can write

$$\bar{n}_0(x) = \int_{-v_0}^{v_0} dv \, P(v) n_0(x, v), \tag{15}$$

where we use $v \equiv v_x$, and for $d = 2$ the distribution of drifts is

$$P(v) = \frac{1}{\pi}\frac{1}{\sqrt{v_0^2 - v^2}}. \tag{16}$$

Even if the drift orientations are uniformly distributed in the variable θ_v, when considering the variable v_x, there is a considerable inhomogeneity with peaks at $v = \pm v_0$.

For the dimension $d = 3$ the disorder-averaged distribution is given by

$$\bar{n}_0(x) = \frac{1}{4\pi}\int_0^{\pi} d\theta_v \int_0^{2\pi} d\phi_v \, \sin\theta_v \, n_0(x, v_0\cos\theta_v) \tag{17}$$

and evaluates to (see Appendix A for the derivation)

$$\bar{n}_0(x) = \frac{1}{2v_0}\int_{-v_0}^{v_0} dv \, n_0(x, v).$$

Comparing to Eq. (15), this implies that $P(v)$ is uniform on the interval $-v_0 \leqslant v \leqslant v_0$,

$$P(v) = \frac{1}{2v_0}. \tag{18}$$

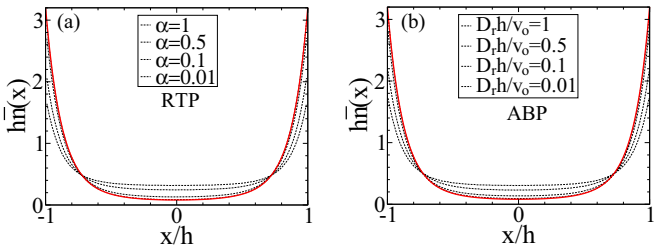

FIG. 2. Distributions of propelled particles between two parallel walls separated by $2h$ obtained from dynamic simulations for $d = 2$ (dashed black lines). The results are for $v_0 h/D = 10$. The solid red line corresponds to the distribution $\bar{n}_0(x)$ in the quenched disorder limit. The results in (a) are for RTP motion and (b) for ABP motion.

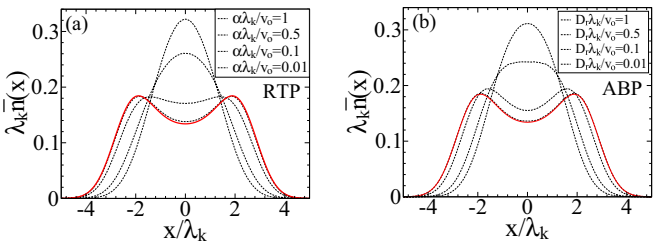

FIG. 3. Distributions of propelled particles in the external potential $u_{\rm ext} = Kx^2/2$ obtained from dynamic simulations for $d = 2$ (dashed black lines). $\lambda_k = \sqrt{2/\beta K}$ is the trap size and the results are for $v_0\lambda_k/D = 5$. The solid red line corresponds to the distribution $\bar{n}_0(x)$. The results in (a) are for RTP and (b) for ABP motion.

The expressions in (16) and (18) show strong dependence of $P(v)$ on the system dimensionality and suggest that the particle deposition at the walls is larger for $d = 2$ than that for $d = 3$.

The next question is, can the integral in (15) be evaluated exactly. Even for uniform distribution $P(v)$, representing the system in $d = 3$, the resulting analytical expression is rather complex. It involves Hurwitz-Lerch ζ and hypergeometric functions. From a practical point of view, it is more convenient to evaluate Eq. (15) numerically for both $d = 2$ and $d = 3$.

In Fig. 2 we show an analogous plot to that in 1 but for particles between two parallel walls and decreasing values of α and D_r in order to demonstrate convergence of the distributions to $\bar{n}_0$. The distribution $\bar{n}_0$ correctly delimits the range within which the distributions n evolve.

A different example of a potential with 1D geometry is the harmonic potential $u_{\rm ext} = \frac{Kx^2}{2}$. The normalized Boltzmann distribution corresponding to the decoupled limit in this case is

$$n_0(x, v) = \sqrt{\frac{\beta K}{2\pi}} e^{-v^2/2\beta K D^2} e^{\frac{vx}{D} - \frac{\beta K x^2}{2}},$$

and the disorder-averaged distribution is obtained from Eq. (15) for an appropriate $P(v)$. For $d = 2$ the integral must be evaluated numerically, and for $d = 3$ it evaluates to the following expression:

$$\bar{n}_0(x) = \frac{D}{2v_0\lambda_k^2}\left(\mathrm{erf}\left[\frac{x}{\lambda_k} + \frac{1}{2}\frac{v_0\lambda_k}{D}\right] - \mathrm{erf}\left[\frac{x}{\lambda_k} - \frac{1}{2}\frac{v_0\lambda_k}{D}\right]\right), \tag{19}$$

where $\mathrm{erf}(x)$ is the error function and $\lambda_k = \sqrt{2/\beta K}$. Unlike the results in (10) and (11), the simple separation between the passive and propelled motion is not possible.

In Fig. 3 we plot the distributions $\bar{n}(x)$ for the potential $u_{\rm ext} = \frac{Kx^2}{2}$ for $d = 2$ for decreasing values of α and D_r, in analogy to Figs. 1 and 2. Once again, the distributions $\bar{n}_0$ correctly delimit the range within which the true distributions for finite α or D_r can be found.

Earlier we briefly discussed the dependence of $P(v)$ on dimensionality when comparing $P(v)$ for $d = 2$ and $d = 3$ in (16) and (18) and the implication of those differences on the accumulation of particles at the trap borders. Below we provide a general expression of $P(v)$, derived in Appendix A, for a general dimension $d > 1$,

$$P(v) = \frac{1}{v_0\sqrt{\pi}}\frac{\Gamma[d/2]}{\Gamma[(d-1)/2]}\left(1 - \frac{v^2}{v_0^2}\right)^{(d-3)/2}, \ \text{if } d > 1, \tag{20}$$

with $P(v)$ normalized and defined on the interval $-v_0 \leqslant v \leqslant v_0$. For $d = 1$ the distribution is represented in terms of δ functions, as drifts in this dimension are limited to two values $v = \pm v_0$ [7],

$$P(v) = \tfrac{1}{2}[\delta(v + v_0) + \delta(v - v_0)], \ \text{ if } \ d = 1. \tag{21}$$

Clearly, the distribution $\bar{n}_0$ calculated using (15) depends on $P(v)$. For large d the distribution $P(v)$ approaches a Gaussian functional form

$$P(v) \approx \sqrt{\frac{d}{2\pi v_0^2}} e^{-\frac{d}{2}(v/v_0)^2},$$

and in the limit $d \to \infty$, $P(v) \to \delta(v)$, and the system loses its quenched disorder—all particles have zero drift, and the system becomes identical with that for passive Brownian particles.

In Fig. 4 we plot the distributions $\bar{n}_0(x)$ for two different external traps, $u_{\rm ext} = \frac{Kx^2}{2}$, and for confinement between two walls, for $P(v)$ in (20) and (21), corresponding to different d. The plots demonstrate strong dependence on d, in particular, they show increased deposition of particles around the trap borders as dimensionality goes down.

A similar dimensionality dependence is found in the opposite limit of large α and/or D_r, accurately represented by the

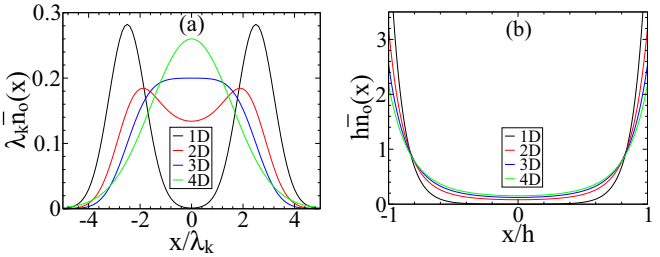

FIG. 4. Distributions $\bar{n}_0(x)$ for an external potential (a) $u_{\rm ext} = Kx^2/2$ and (b) for particles between two walls, for different system dimensionality d. The distributions are for $v_0\lambda_k/D = 5$ and $v_0 h/D = 10$.

concept of effective temperature [12,13,14] valid for $d > 1$,

$$\frac{T_{\rm eff}}{T} = 1 + \frac{1}{d(d-1)}\frac{v_0^2}{D(\alpha + D_r)}, \tag{22}$$

where increased dimensionality d brings $T_{\rm eff}$ closer to thermodynamic temperature T. In the limit $d \to \infty$, $T_{\rm eff} = T$. The reason for this behavior is rather simple. The constant velocity v_0 and the associated kinetic energy is distributed into d components. For increased dimensionality, the extra kinetic energy that goes to each degree of freedom is reduced, giving rise to the observed cooling effect.

IV. SELF-CONSISTENT FORMULATION

The next step is to try to expand the distribution n around the decoupled limit as $n \approx n_0 + \alpha n_1$. However, such a systematic expansion yields expressions which are complex and not very insightful. Instead, we reformulate the stationary FP equation as a self-consistent relation (SC). The resulting formulation yields interesting insights, provides a basis for an alternative computation of distributions, and can be used for obtaining perturbative expansion of n.

A. RTP particles

To keep things simple, we consider a system with 1D geometry. For the RTP motion the stationary FP equation in 1D can be written as

$$0 = Dn'' + \beta D[u'_{\rm eff} n]' + \alpha(\bar{n} - n),$$

where the effective potential incorporates the drift as $\beta u_{\rm eff} = \beta u_{\rm ext} - \frac{v}{D}x$, and the disorder-averaged distribution is $\bar{n} = \int dv\, P(v) n(n, x)$. The same equation can be written as

$$0 = n'' + \beta[u'_{\rm eff} n]' + s, \tag{23}$$

where

$$s = \frac{\alpha}{D}(\bar{n} - n) \tag{24}$$

plays the role of the source function. Note that the source function satisfies $\int dx\, s(x, v) = 0$ and $\int dv\, P(v) s(x, v) = 0$.

By introducing the source function, Eq. (6) can be regarded as an inhomogeneous second-order differential equation. The solution then can be obtained using the method of variation of parameters. To proceed, we first need solutions for the homogenous equation. The two possible solutions are

$$y_0 = e^{-\beta u_{\rm eff}}, \quad y_1 = y_0 Y_0, \tag{25}$$

where

$$Y_0 = \int dx\, e^{\beta u_{\rm eff}}. \tag{26}$$

The first solution corresponds to the Boltzmann distribution. The second solution is normally rejected on physical grounds due to its nonvanishing local flux, $D\rho' + u'_{\rm eff}\rho \neq 0$, when dealing with passive particles. As we will see, this solution becomes relevant for describing propelled particles.

The solution of the second-order inhomogeneous equation can be expressed as

$$n = Ay_0 + By_1 + \left[y_0 \int dx\, \frac{y_1}{w} s - y_1 \int dx\, \frac{y_0}{w} s \right], \tag{27}$$

where A and B are undefined coefficients, and $w = y_0 y_1' - y_0' y_1$ is the Wronskian that for the present case evaluates as $w = y_0$. The first two terms constitute a complementary solution, and the last term is the particular solution. Since the second term does not produce a vanishing flux, B is set to zero. After using (25) and substituting (24) for the source function, the solution transforms into the desired SC relation,

$$n = Ae^{-\beta u_{\rm eff}} + \frac{\alpha e^{-\beta u_{\rm eff}}}{D}\left[\int dx\, (\bar{n} - n) Y_0 - Y_0 \int dx\, (\bar{n} - n) \right], \tag{28}$$

where A is determined from the condition of normalization $\int_L dx\, n(x, v) = 1$ on the domain L prescribed by a physical problem. Note that for $\alpha = 0$, we recover $n = n_0$.

The SC relation in (28) reveals a certain mean-field character of the formulation [15] and the presence of the effective interactions between particles—particles appear to be "attracted" toward the average distribution $\bar{n}$. The origin of this coupling between particles, however, is different from that in a system of truly interacting particles. It is caused by the "reaction" part of the FP equation, as particles of different drift, regarded as belonging to different species, exchange their identity.

If the RTP particles are confined between two parallel walls, then $\beta u_{\rm eff} = -\frac{vx}{D}$ and

$$Y_0 = -\frac{D}{v} e^{-\frac{vx}{D}},$$

and the SC relation becomes

$$n = An_0 + \alpha \int_{-h}^{x} dx' \left[\frac{1 - e^{\frac{v}{D}(x - x')}}{v} \right] (\bar{n} - n). \tag{29}$$

The above SC relation is next used as a basis for numerical computation of the distributions n based on iterative procedure starting with n_0. For $\alpha \geqslant 0.5$ a mixing parameter is used, $0 < \gamma < 1$, for generating the next distribution as $n_{\rm new} \equiv (1 - \gamma) n_{\rm old} + \gamma n_{\rm new}$. For the bin size $\Delta x = 0.01$ the convergence is attained within 10–20 iterations (amounting to a few seconds of the CPU time, a significant improvement over dynamic simulations).

Figure 5 plots the numerically calculated stationary distributions for $d = 2$ [using the distribution $P(v)$ in (16)]. The distributions are in perfect correspondence with those obtained from dynamic simulations.

The SC formulation in (28), or that for particles between walls in (29), can also be used for constructing subsequent terms within the perturbative approach, $n = n_0 + \alpha n_1 + \cdots$, by inserting n_0 on the right-hand side of those equations. If considering Eq. (29) we get

$$n_1 = \int_{-h}^{x} dx' \left[\frac{1 - e^{\frac{v}{D}(x - x')}}{v} \right] (\bar{n}_0 - n_0) + Cn_0, \tag{30}$$

where the constant C is such as to ensure the condition $\int_{-h}^{h} dx\, n_1(x, v) = 0$, since the perturbation n_1 cannot create or destroy particles, only redistribute them in the interval $-h \leqslant x \leqslant h$. We recall that $n_0(x, v)$ for the system between walls is given in Eq. (13); however, inserting this expression into (30) does not lead to analytical results, and the perturbative formulation itself does not shed any additional light.

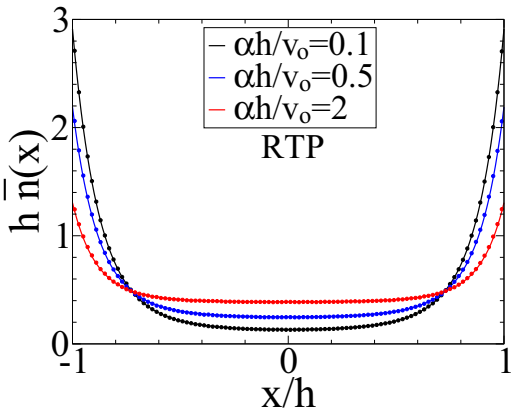

FIG. 5. Distributions $\bar{n}(x)$ obtained numerically using the SC formulation of the FP equation for the RTP particles between two walls for $d = 2$ and $v_0 h/D = 10$. Circles correspond to simulation data points.

We next consider a harmonic potential, in which case $\beta u_{\rm eff} = -\frac{vx}{D} + \frac{\beta K x^2}{2}$,

$$Y_0 = \frac{\lambda_k\sqrt{\pi}}{2} e^{-(\frac{v\lambda_k}{2D})^2} \mathrm{erfi}\Big[\frac{x}{\lambda_k} - \frac{1}{2}\frac{v\lambda_k}{D}\Big],$$

where $\mathrm{erfi}(x) = -i\mathrm{erf}(ix)$ is the imaginary error function, and the SC equation expressed in terms of definite integrals is

$$ne^{\beta u_{\rm eff}} = A + \frac{\alpha}{D}\Big[\int_{-\infty}^{x} dx'\,(\bar{n} - n)Y_0 - Y_0\int_{-\infty}^{x} dx'\,(\bar{n} - n)\Big]. \tag{31}$$

For numerical integration the limits $x = \pm\infty$ are substituted by $x = \pm x_c$, where the cutoff distance x_c is large enough so that $n(\pm x_c, v) \approx 0$. Numerically calculated distributions for $d = 2$ are shown in Fig. 6. Again, the distributions are in perfect correspondence with those obtained from dynamic simulations.

B. ABP particles

A self-consistent relation could similarly be established for the ABP type of motion. Considering the system dimension

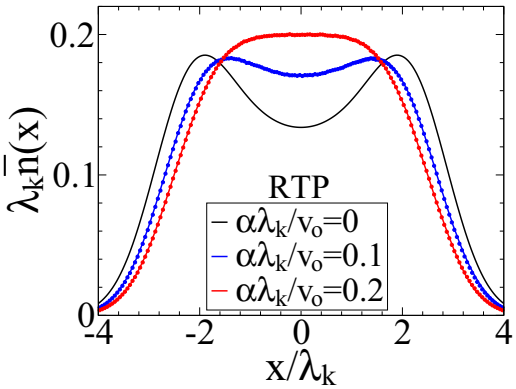

FIG. 6. Distributions $\bar{n}(x)$ obtained numerically using the SC formulation for the RTP particles in the potential $u_{\rm ext} = Kx^2/2$ for $d = 2$ and $v_0\lambda_k/D = 5$. Circles correspond to simulation data points.

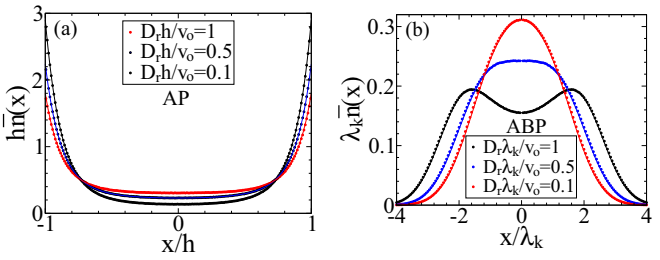

FIG. 7. Distributions $\bar{n}(x)$ obtained numerically from the SC formulation for the ABP particles for $d = 2$ (a) between two walls with $v_0 h/D = 10$ and (b) in the harmonic potential with $v_0\lambda_k/D = 5$. Circles correspond to simulation data points.

$d = 2$ and a system with 1D geometry, the stationary FP equation that describes this situation, obtained using Eq. (2) with $\alpha = 0$ but for finite D_r, is

$$0 = n'' + \beta D[u'_{\rm eff} n]' + \frac{D_r}{D}\frac{\partial^2 n}{\partial\theta_v^2}, \tag{32}$$

where $n \equiv n(x, \theta_v)$. If the source term is defined as

$$s = \frac{D_r}{D}\frac{\partial^2 n}{\partial\theta_v^2},$$

we arrive at a similar form to that in (23) and can follow up with the same procedure. In the case of ABP motion, the expressions are more economic if the distributions are defined in terms of θ_v rather than $v \equiv v_x$.

The SC relation that follows is

$$n = Ae^{-\beta u_{\rm eff}} + \frac{D_r e^{-\beta u_{\rm eff}}}{D}\Big[\int dx\, Y_0\,\frac{\partial^2 n}{\partial\theta_v^2} - Y_0\int dx\,\frac{\partial^2 n}{\partial\theta_v^2}\Big] \tag{33}$$

and can next be used as a basis for calculating stationary distributions. The results are shown in Fig. 7. Unlike for the RTP particles, the numerical method is less robust and a larger number of iterations are required to reach convergence.

V. WHAT IS THE TRUE EQUILIBRIUM?

There is an interesting consequence of treating the system at $\alpha = D_r = 0$ as a reference point and considering deviations from it as a "distance" from equilibrium. According to this viewpoint, the system at $\alpha \to \infty$ or $D_r \to \infty$, represents the largest deviation—the conclusion that runs counter to the more accepted view that regards as a reference state (and equilibrium) the limit $\alpha \to \infty$ or $D_r \to \infty$.

One way to resolve this controversy, of which reference point corresponds to equilibrium, is to resort to the arbitration of the entropy production, considered as a sophisticated way of quantifying the degree of violation of detailed-balance condition. We will not make calculations for the entropy production for our system. Instead we use the exact expression for the RTP system in $d = 1$, where for $P(v) = \frac{1}{2}[\delta(v - v_0) + \delta(v + v_0)]$, found in Ref. [7] in Eq. (17) and given by

$$\Pi = \alpha\frac{hk\cosh hk - \sinh hk}{\frac{\alpha D}{v_0^2}hk\cosh hk + \sinh hk}, \tag{34}$$

where $k = \frac{v_0}{D}\sqrt{1+\frac{\alpha D}{v_0^2}}$. In true equilibrium, $\Pi = 0$. The larger the value of Π, the larger the deviation from equilibrium. If we plot Π as a function of α for fixed D and v_0 we discover that $\Pi(\alpha = 0) = 0$, and as α increases Π grows monotonically and in the limit $\alpha \to \infty$ we have $\Pi(\alpha \to \infty) = \frac{v_0^2}{D}$. Such a result appears to vindicate our viewpoint that the "correct" equilibrium corresponds to the decoupled limit, not the other way around. The reason for this surprising result is that even if the distribution n becomes flat and the transport due to diffusion vanishes, a convective type of motion is still there.

VI. CONCLUSION

This work starts by recognizing that at the precise condition $\alpha = D_r = 0$, where orientation of the drifts becomes fixed and time independent, the system attains an equilibrium with quenched disorder. This intuitive interpretation permits us to obtain exact stationary distributions of propelled particles in confining potentials. The central quantity that emerges is the effective potential $u_{\rm eff}$, which is the sum of an external potential and a linear potential for representing drift, and the Boltzmann factor $e^{-\beta u_{\rm eff}}$.

In the second part of this work we construct the theoretical framework in which the decoupled state figures naturally. This is done by reformulating the stationary FP equation as a self-consistent relation, formulated in terms of the Boltzmann factor $e^{-\beta u_{\rm eff}}$. The formulation reveals the presence of coupling between propelled particles (even if there are no true interactions between particles) as a result of a "chemical" process whereby particles with different drift are represented as different species that continuously exchange identities. The self-consistent formulation is used as a basis for numerical computation of stationary distributions, as an alternative to dynamic simulations. The SC formulation can also be used to expand n perturbatively around n_0.

The viewpoint that considers the decoupled condition as an equilibrium state raises the question, So what is the real equilibrium? Generally, equilibrium is attributed to the limit $\alpha \to \infty$ and/or $D_r \to \infty$, since the distribution in those limits converges to that of passive Brownian particles. However, if we look into the entropy production Π that is supposed to measure a distance from equilibrium, we get the results that support the case for the decoupled limit as a true equilibrium.

The data that support the findings of this study are available from the corresponding author upon reasonable request.

ACKNOWLEDGMENTS

D.F. acknowledges financial support from FONDECYT through Grant No. 1201192. D.F. thanks the University of Tel Aviv for invitation under the program "Visiting Scholar of The School of Chemistry."

APPENDIX: DISTRIBUTIONS $P(v)$ FOR A GENERAL d DIMENSION

A general, disorder-averaged distribution over drift orientations uniformly distributed on the surface of a unit sphere in d dimension for the system with 1D geometry, such as a system between two parallel walls or in the harmonic potential $u_{\rm ext} = \frac{Kx^2}{2}$, is

$$\bar{n}_0(x) \propto \int_0^{2\pi} d\Omega_v \, n_0(x, v_0 \cos\theta_v),$$

where $v_x = v_0 \cos\theta_v$ is the velocity component in the direction perpendicular to the boundaries of a trap. The stationary distribution is uniform in the remaining directions.

Since for an arbitrary dimension d, $d\Omega$ is defined as

$$d\Omega = \sin^{d-2}\varphi_1 \sin^{d-3}\varphi_2 \cdots \sin d\varphi_{d-2}\, d\varphi_1\, d\varphi_2 \cdots d\varphi_{d-1},$$

where $\theta = \varphi_1$, we may write

$$\int d\Omega_v \, n_0(x, v_0\cos\theta_v) \propto \int_0^{\pi} d\theta_v \, \sin^{d-2}\theta_v \, n_0(x, v_0\cos\theta_v),$$

as the angles φ_k for $k > 1$ can be ignored. The above integral is transformed using $d\theta_v = -\frac{1}{v_0}\frac{dv}{\sin\theta_v}$, where $v \equiv v_0\cos\theta_v$, and $\sin\theta_v = \sqrt{1-\cos^2\theta_v}$ into

$$\int d\Omega_v \, n_0(x, v_0\cos\theta_v) \propto \int_{-v_0}^{v_0} dv \left(1-\frac{v^2}{v_0^2}\right)^{\frac{d-3}{2}} n_0(x, v),$$

and the normalized distribution $P(v)$ for an arbitrary dimension d is

$$P(v) = \frac{1}{v_0\sqrt{\pi}} \frac{\Gamma\left[\frac{d}{2}\right]}{\Gamma\left[\frac{d-1}{2}\right]} \left(1-\frac{v^2}{v_0^2}\right)^{\frac{d-3}{2}}. \tag{A1}$$

[1] M. J. Schnitzer, Theory of continuum random walks and application to chemotaxis, Phys. Rev. E **48**, 2553 (1993).

[2] J. Tailleur and M. E. Cates, Statistical Mechanics of Interacting Run-and-Tumble Bacteria, Phys. Rev. Lett. **100**, 218103 (2008).

[3] J. Tailleur and M. E. Cates, Sedimentation, trapping, and rectification of dilute bacteria, Europhys. Lett. **86**, 60002 (2009).

[4] L. Angelani, Confined run-and-tumble swimmers in one dimension, J. Phys. A: Math. Theor. **50**, 325601 (2017).

[5] K. Malakar, V. Jemseena, A. Kundu, K. V. Kumar, S. Sabhapandit, S. N. Majumdar, S. Redner, and A. Dhar, Steady state, relaxation and first-passage properties of a run-and-tumble particle in one-dimension, J. Stat. Mech.: Theory Exp. (2018) 043215.

[6] A. Dhar, A. Kundu, S. N. Majumdar, S. Sabhapandit, and G. Schehr, Run-and-tumble particle in one-dimensional confining potentials: Steady-state, relaxation, and first-passage properties, Phys. Rev. E **99**, 032132 (2019).

[7] N. Razin, Entropy production of an active particle in a box, Phys. Rev. E **102**, 030103(R) (2020).

[8] U. Basu, S. N. Majumdar, A. Rosso, S. Sabhapandit, and G. Schehr, Exact stationary state of a run-and-tumble particle with three internal states in a harmonic trap, J. Phys. A: Math. Theor. **53**, 09LT01 (2020).

[9] D. Martin, J. O'Byrne, M. E. Cates, É. Fodor, C. Nardini, J. Tailleur, and F. van Wijland, Statistical mechanics of active Ornstein-Uhlenbeck particles, Phys. Rev. E **103**, 032607 (2021).

[10] D. Martin and T. A. de Pirey, AOUP in the presence of Brownian noise: A perturbative approach, arXiv:2009.13476.

[11] D. Frydel and R. Podgornik, Mean-field theory of active electrolytes: Dynamic adsorption and overscreening, Phys. Rev. E **97**, 052609 (2018).

[12] A. P. Solon, Y. Fily, A. Baskaran, M. E. Cates, Y. Kafri, M. Kardar, and J. Tailleur, Pressure is not a state function for generic active fluids, Nat. Phys. **11**, 673 (2015).

[13] L. Berthier and J. Kurchan, Non-equilibrium glass transitions in driven and active matter, Nat. Phys. **9**, 310 (2013).

[14] G. Szamel, Self-propelled particle in an external potential: Existence of an effective temperature, Phys. Rev. E **90**, 012111 (2014).

[15] D. Frydel, Mean field electrostatics beyond the point charge description, Adv. Chem. Phys. **160**, 209 (2016).